Available online at www.sciencedirect.com
ScienceDirect
Trans. Nonferrous Met. Soc. China 32(2022) 1351−1361
Transactions of Nonferrous Metals Society of China
www.tnmsc.cn

Preparation of low-oxygen-containing Ti−48Al−2Cr−2Nb alloy powder by direct reduction of oxides

Xue-yi GUO, Zhao-wang DONG, Yang XIA, Pei-dong LIU, Han-ning LIU, Qing-hua TIAN

School of Metallurgy and Environment, Central South University, Changsha 410083, China

Received 28 January 2021; accepted 26 September 2021

Abstract: A high-purity Ti−48Al−2Nb−2Cr alloy powder with an oxygen content as low as 0.0572 wt.% and a particle size of <150 μm was produced from a mixture of TiO_2, Al_2O_3, Nb_2O_5, and Cr_2O_3 powders through reduction with magnesium and deoxidation with calcium. The phase and composition of the products were analyzed. The final product mainly included γ-TiAl and minor α_2-Ti_3Al phases, and Ti, Al, Cr, and Nb were homogenously distributed in the powder with a mole ratio of 49.73:43.51:2.05:1.98. The reduction and deoxidation mechanisms were investigated by thermodynamic modeling using the HSC Chemistry software and Pandat software based on the Ti alloy database.
Key words: titanium aluminide; powder; reduction; oxide

1 Introduction

γ-TiAl-based alloys have attracted garnered considerable interest for applications in the aerospace, marine, energy, and chemical industries owing to their high melting point, low density, high specific strength, and good resistance to both oxidation at high temperature and corrosion [1−4]. However, their low room-temperature plasticity and poor processing and formability have severely restricted their widespread application [5,6]. Powder metallurgy (PM) is regarded as a promising method for producing TiAl-based alloys because it offers near-net shape fabrication, uniform composition, fine microstructures, and high material utilization. Furthermore, it avoids casting defects such as porosity and shrinkage cavities [7−10]. Powder production and powder consolidation are the two most important aspects of powder metallurgy for TiAl-based alloys. The consolidation of TiAl-based alloys has significantly advanced over the last few decades [11−15], but recently, the focus of research on these alloys has shifted to powder production [16−20].

Traditionally, TiAl alloy powders are produced by atomization methods, including inert gas atomization (GA), plasma rotating electrode process (PREP), and plasma atomization [21−23]. These methods have disadvantages of low yield of powder with a desirable particle size and high energy consumption, leading to a high cost. Researchers have attempted various methods for preparing low-cost pre-alloyed TiAl powders. MWAMBA and CHOWN [24] produced TiAl powder through mechanical alloying (MA). This is a simple and facile method for obtaining low-cost products, but during the ball-milling process, it is difficult to avoid impurities and oxidation inclusions. NOVÁK et al [25] successfully prepared TiAl−xSi alloy powder through a self-propagating high-temperature synthesis (SHS) process, which

The authors Xue-yi GUO and Zhao-wang DONG contributed equally to this work
Corresponding author: Yang XIA, Tel: +86-17307415033, E-mail: yang.xia@csu.edu.cn
DOI: 10.1016/S1003-6326(22)65858-8

has the advantages of simple operation and short synthesis cycle. Unfortunately, this method results in a high impurity content, especially interstitial elements such as oxygen.

In recent years, some scholars have proposed thermochemical methods for preparing TiAl alloys. BOUDEBANE et al [26] prepared Ti_3Al intermetallic powder by the reduction of TiO_2−Al_2O_3 oxides with calcium or magnesium, thus obtaining a Ti−Al alloy powder consisting of TiAl and Ti_3Al phases and 0.9 wt.% oxygen. MAEDA et al [27] employed the aluminothermic reduction of TiO_2 in an argon atmosphere to produce a TiAl powder with 1.5 wt.% oxygen content. SONG et al [28] prepared TiAl alloy powder using TiO_2 as the raw material, Al as the reducing agent, and Ca as the deep reducing agent. The final powder contained 58.36 wt.% Ti, 40.19 wt.% Al, and 1.41 wt.% oxygen. SUZUKI et al [29−31] studied the preparation of TiAl alloy through the calciothermic reduction of oxides. Specifically, they used CaH_2 to produce a porous structured powder with only 0.12 wt.% oxygen. However, to the best of the authors' knowledge, no reported studies have achieved a dense TiAl powder with <0.1 wt.% oxygen, which is desirable for powder metallurgy applications. Thermochemical processes usually produce porous TiAl powder with a high oxygen content, and the reduction mechanism and reduction sequence during these processes have not yet been clearly identified.

This paper presents a thermochemical method for preparing TiAl alloy powder by directly reducing metal oxides via a two-step gradient reduction process. The major reduction step used magnesium to remove most of the oxygen. Then, a small amount of calcium, which is more expensive but a stronger reducing agent than magnesium, was used in the second reduction step to remove the remaining oxygen. Between the two reductions, a heat-treatment step was designed to control the particle size and specific surface area of the powder. Using this process, a TiAl alloy powder with an oxygen content of 0.0572 wt.% was prepared using a mixture of TiO_2, Al_2O_3, Nb_2O_5, and Cr_2O_3 powders as the raw material. The powders were characterized in detail at each step, and the reduction and deoxidation mechanisms were investigated.

2 Experimental

The process flowchart is presented in Fig. 1. The raw materials used in this study were chemically pure TiO_2 (60−80 nm), Al_2O_3 (5−6 μm), Nb_2O_5 (30−50 nm), and Cr_2O_3 (10−20 μm) powders (Aladdin Ltd.). In the first reduction step, anhydrous magnesium chloride ($MgCl_2$) powder was used as the flux, and Mg metal powder with a particle size between 80−150 μm (Sinopharm Chemical Reagent Co. Ltd.) was used as the reducing agent. In the subsequent deoxidation step, calcium chloride (Aladdin Ltd.) and calcium granules (1−2 mm) were used as the flux and reducing agents, respectively. First, 10 g of TiO_2 was weighed, and the masses of Al_2O_3, Cr_2O_3, and Nb_2O_5 were then calculated according to the atomic ratio of Ti, Al, Cr, and Nb in the Ti−48Al−2Cr−2Nb alloy. The TiO_2, Al_2O_3, Cr_2O_3, and Nb_2O_5 powders, anhydrous $MgCl_2$ powder, and the Mg powder were mixed in a specific ratio for 15 min, loaded into a molybdenum crucible, and then fed into a tube furnace (TF14P80 TAISITE) for reduction. The mixture was heated to 750 °C and held for 4 h in an argon atmosphere at a flow rate of 1 L/min. The reduced product was then cooled to room temperature. The product was placed in a beaker to form a slurry with deionized (DI) water, and acetic acid was added gradually, maintaining the pH of the slurry between 3 and 5. After acid leaching, the undissolved powder was washed with ultrapure water and anhydrous ethanol and filtered, and then

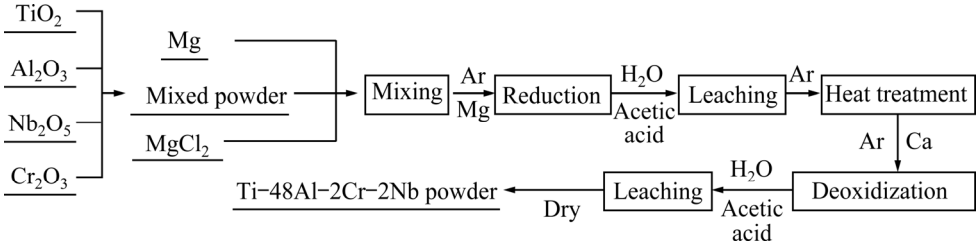

Fig. 1 Process flowchart for preparation of Ti−48Al−2Cr−2Nb alloy powders

dried in a drier at 50 °C. The dried powder was placed in a molybdenum crucible and heated to 1000−1400 °C in a tube furnace for 2 h in an argon atmosphere. After cooling, the powder was milled to a size of 150 μm for further deoxidation. The heated powder, anhydrous $CaCl_2$ powder, and granular calcium were mixed at a specific ratio for 15 min and then placed in a molybdenum crucible and heated to 900 °C in a tube furnace for 8−12 h. Ca was used for the deoxidation process, and lastly, the deoxidized product was leached with acetic acid and DI water and dried to obtain the final powder.

The raw material, intermediate product, and final powder were characterized by inductively coupled plasma-atomic emission spectrometry (ICP-AES, Optima5300), scanning electron microscopy (SEM) equipped with energy-dispersive spectroscopy (EDS), and X-ray diffraction (XRD). The oxygen content in the powder was determined using an oxygen and nitrogen analyzer (LECO TCH600). The specific surface area of the powder at each step was determined using Brunauer–Emmett–Teller (BET) surface area measurement (JW-BK222). The particle size distribution of the final powder was measured using a laser particle size analyzer (Mastersize 2000). For all composition analyses, standard materials were used for calibration. Each sample was tested three times, and the average value was used for further analysis. Error bars were calculated from these triplicate multiple results. To better understand the reduction mechanism, detailed thermodynamic modeling was conducted with the help of two commercial software programs, HSC Chemistry software [32] and Pandat thermodynamic software, along with a Ti alloy database [33].

3 Results and discussion

3.1 Powder characterization

The mixture of TiO_2, Al_2O_3, Cr_2O_3, and Nb_2O_5 powders was reduced by Mg, leached by acetic acid, heat treated in argon, and then deoxidized by calcium. The raw material and products were characterized at each step, and the results are shown in Fig. 2. The mass fractions of Ti, Al, Cr, Nb, and O were determined to be 34.35%, 19.35%, 1.54%, 2.77% and 41.99% (mass fraction), respectively. As shown in Fig. 2(b), after the first reduction, the Ti content increased to 60.4%, while the ratio of Ti to

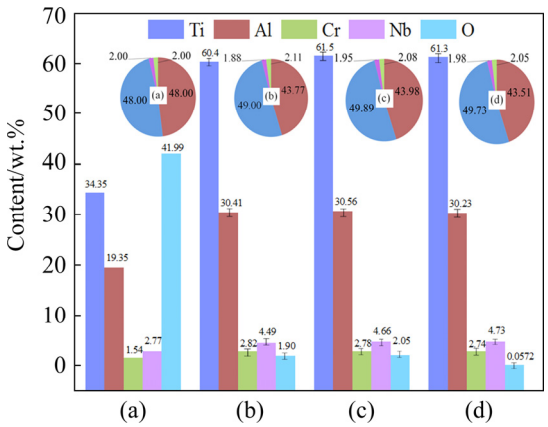

Fig. 2 Composition of raw material and product at each step (The pie charts showing mole fraction of all elements except oxygen): (a) Mixed raw materials; (b) Reduced powder; (c) Heat-treated powder; (d) Deoxidized powder

Al changed from 48.00:48.00 to 49.00:43.77, which indicated that a small amount of Al was lost. This slight decrease may be due to the first leaching step with acetic acid. In addition, the Cr and Nb contents slightly changed to 2.82% and 4.49% respectively. After this first reduction and leaching step, the mole ratio of Ti, Al, Cr, and Nb was determined to be 49.00:43.77:2.11:1.88. Figure 2(b) also shows that the oxygen content was successfully decreased to 1.90% after the first reduction; then, it slightly increased to 2.05% after the heat treatment step (Fig. 2(c)), which may be due to environmental oxygen. The mole ratios of Ti, Al, Cr, and Nb remained essentially the same after the heat treatment and deoxidation steps. Notably, the deoxidation step decreased the oxygen content in the final product to be as low as 0.0572%, which was much lower than the standard specifications for oxygen in titanium sponge (0.15%, ASTM B299) and in γ-TiAl (Ti−48Al−2Cr−2Nb) (0.12%, AMS 7023).

Figure 3 shows the product morphology at each step. The reduced powder had an irregular and porous morphology and contained many fine particles. Figures 3(b) and (c) indicate that the heat treatment coarsened the powder and produced irregular, dense particles with some minor internal pores, and the deoxidation step effectively maintained the morphology of the heat-treated powder. The particle size distribution of the final powder was analyzed using a laser particle size

analyzer, as shown in Fig. 4. The d_{10}, d_{50}, and d_{90} values of the final product were 37.72, 67.19, and 115.51 μm, respectively. Figure 4(b) illustrates the changes in the volume average particle diameter and specific surface area of the products at each step. Clearly, the heat treatment considerably decreased the specific surface area of the powder, which was not significantly affected by the deoxidation step. The specific surface area of the final product was 0.29 m^2/g, which was close to that of the heat-treated powder. The particles in the deoxidized powder were smaller than those in the heat-treated powder, which was probably because of the gentle grinding effect during stirring of the leaching solution. The decreased specific surface area is beneficial to controlling the oxygen content in the powder as an oxide layer is always present on the powder surface.

3.2 Distribution and evolution of alloying elements

The elemental distribution of the powders was analyzed in detail after each step with the assistance of elemental EDS mapping, and the results are shown in Figs. 5−7. After the first reduction at 750 °C (Fig. 5), Ti and Al were homogenously distributed, indicating that Ti and Al might have alloyed, but Nb and Cr agglomerated and did not diffuse into the alloy during the reduction step. The elemental distribution of the powder after heat treatment at 1300 °C for 2 h (Fig. 6) shows that most of Cr and Nb diffused into the TiAl, but some of Cr and Nb remained segregated and formed Cr- and Nb-enriched islands. Nevertheless, most of elements were uniformly distributed after the heat treatment step overall. The EDS mapping of the deoxidized product in Fig. 7 reveals that the deoxidation step did not change the elemental distribution because a low temperature was used (900 °C). The reduced powder had an oxygen level as high as 1.9%, which may affect the sintering response of the powder. After the deoxidation step, the oxygen content was decreased to 0.057%, which would be advantageous to sintering, as a powder with a lower oxygen level can result in a higher density at the same sintering temperature.

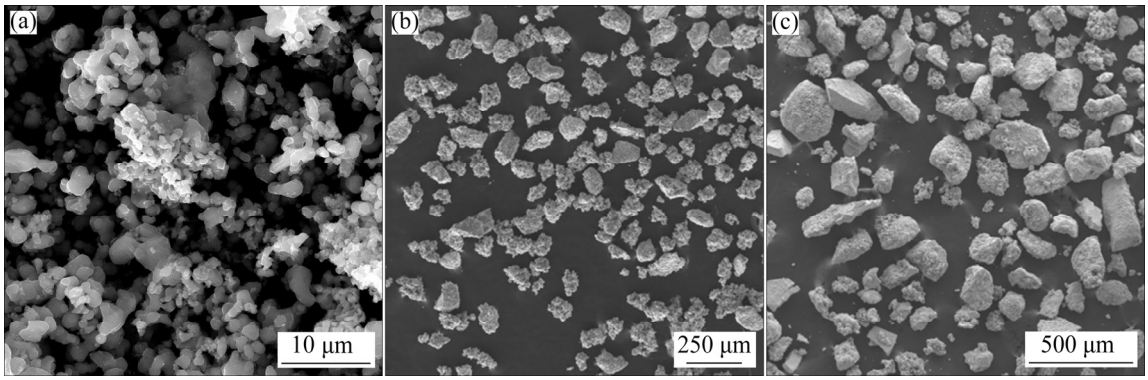

Fig. 3 SEM images of products at each step: (a) Reduction; (b) Heat-treatment; (c) Deoxidization

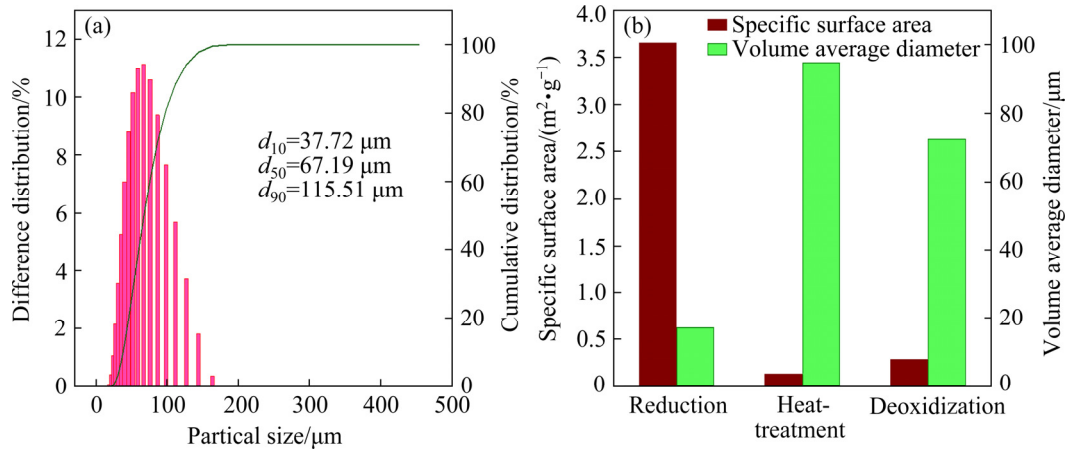

Fig. 4 Particle size distribution of final products (a); Volume average diameter and specific surface area of products at each step (b)

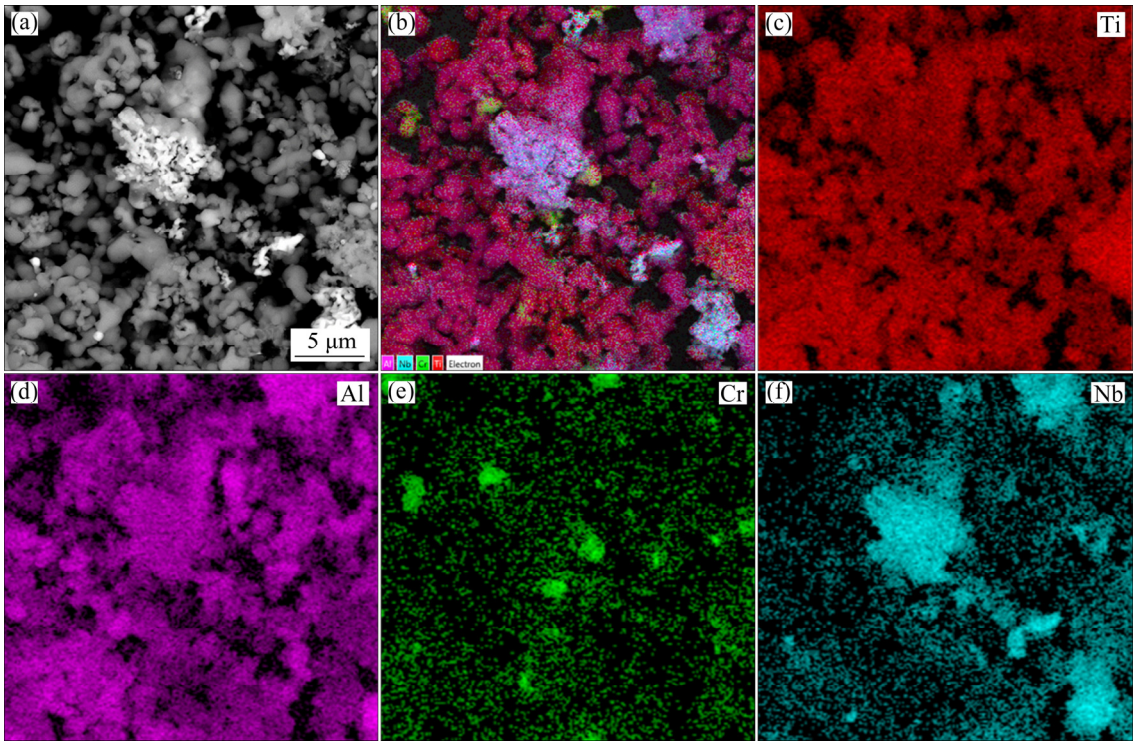

Fig. 5 EDS elemental mappings of reduced powder

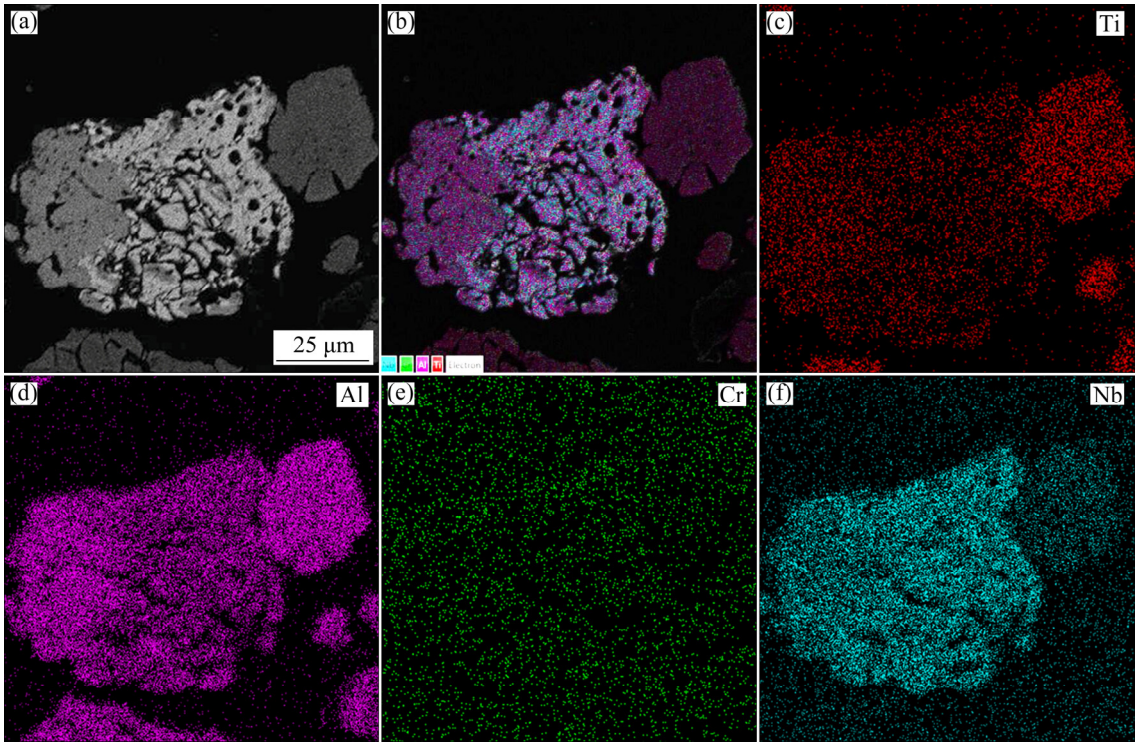

Fig. 6 EDS elemental mappings of heat-treated powder

To clarify the phase changes during the entire process, XRD analysis was conducted for the product powder after each step. As shown in Fig. 8, the raw material was a mixture of TiO_2, Al_2O_3, Nb_2O_5, and Cr_2O_3 in proportion to the target Ti−48Al−2Cr−2Nb alloy. After the mixed powder was reduced by Mg, the major phases of MgO, γ-TiAl, α_2-Ti_3Al, and excess Mg were detected in the reduced and unleached products. After acid leaching, magnesium oxide and magnesium were

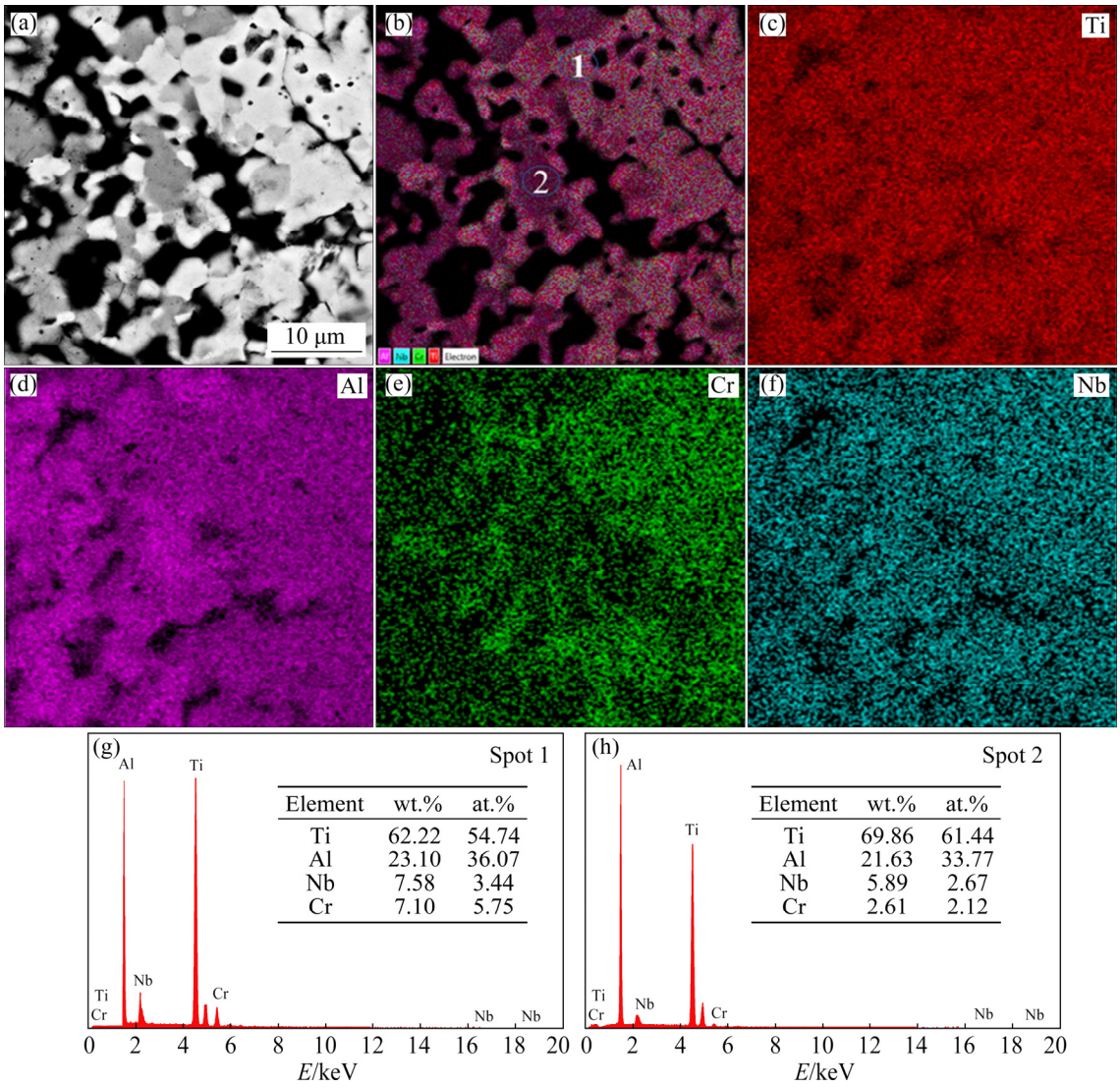

Fig. 7 EDS elemental mappings and point analysis of deoxidized powder

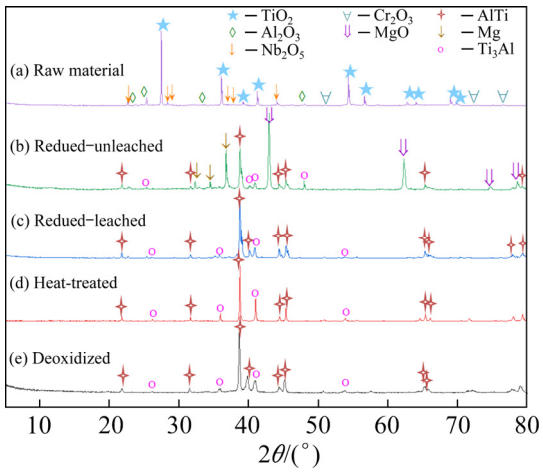

Fig. 8 XRD patterns of raw material and products at each step: (a) Mixed raw materials; (b) Reduced and unleached; (c) Reduced and leached; (d) Heat-treated; (e) Deoxidized

absent. The XRD patterns of the heat-treated and deoxygenated powders were similar, and both contained γ-TiAl and α_2-Ti_3Al phases.

3.3 Mechanism of reduction and deoxidation

A thermodynamic model of the reduction system was constructed to understand the reduction mechanism. In the Ellingham diagram of MgO and other oxides (Fig. 9), TiO_2, TiO, Al_2O_3, Cr_2O_3, and Nb_2O_5 exhibit higher oxygen potentials than MgO, indicating that they can be easily reduced by Mg in the temperature range of 100−1300 °C. This modeling thus suggests that Mg is a suitable reducing agent for mixed oxides during the first reduction. Figure 10 presents the equilibrium composition diagram produced by HSC Chemistry software with inputs of 0.125 kmol TiO_2,

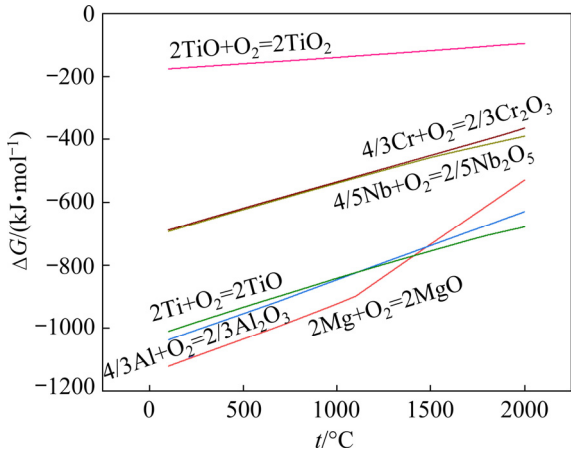

Fig. 9 Thermodynamic modelling of reactions during reduction

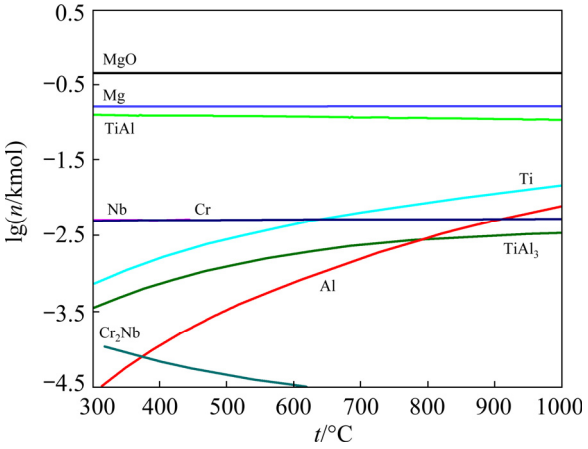

Fig. 10 Equilibrium composition diagram with inputs of 0.125 kmol TiO_2, 0.0625 kmol Al_2O_3, 0.0026 kmol Nb_2O_5, 0.0026 kmol Cr_2O_3, and 0.5 kmol Mg produced by HSC Chemistry software

0.0625 kmol Al_2O_3, 0.0026 kmol Nb_2O_5, 0.0026 kmol Cr_2O_3, and 0.5 kmol Mg. This diagram indicates that Mg metal has a strong thermodynamic driving force to reduce all oxides, and no other oxides of titanium are formed. Indeed, the main substances produced in the reaction system are MgO, intermetallic compound TiAl, and excess magnesium. The reduction may proceed as the following equations:

$$TiO_2+2Mg=Ti+2MgO \quad (1)$$

$$Al_2O_3+3Mg=2Al+3MgO \quad (2)$$

$$Cr_2O_3+3Mg=2Cr+3MgO \quad (3)$$

$$Nb_2O_5+5Mg=2Nb+5MgO \quad (4)$$

$$2Al+4Ti=TiAl+Ti_3Al \quad (5)$$

In fact, the reduction of TiO_2 by magnesium is a SHS process. Specifically, a significant amount of heat is generated during the reduction reaction, as reported by some researchers [34,35]. Some excess magnesium particles were observed to be condensed on one side of the tube, where the actual reaction temperature might be higher than the set temperature (750 °C). The formation of Ti_3Al and TiAl instead of $TiAl_3$ confirmed that the reaction temperature was actually much higher than 750 °C because at such a low temperature, it is impossible to form Ti_3Al and TiAl phases [36−38]. In addition, the partial dissolution of Cr and Nb into the TiAl matrix also suggested that the reduction reaction occurred at a high temperature, which dissolved Cr and Nb, as shown in Fig. 5. The Mg content in the products at each step (Table 1) suggested that Mg was not completely leached out of the reduced powder after the acid leaching step. No Mg was detected by EDS in the heat-treated powder, which is probably because the Mg content was lower than the detection limit of EDS. Thermodynamic calculations were performed on the Al−Mg and Al−Ti systems using Pandat software, and the results were shown in Fig. 11. Evidently, in the temperature range of 300−1000 °C, TiAl and Ti_3Al are much more stable than A_2Mg_3 or $Al_{12}Mg_{17}$, suggesting that A_2Mg_3 or $Al_{12}Mg_{17}$ may not have formed during the reduction step.

Table 1 ICP-OES results of Mg content in powder at each step

Powder	Content of Mg/%
Reduced	0.43
Heat-treated	0.098
Deoxidized	0.061

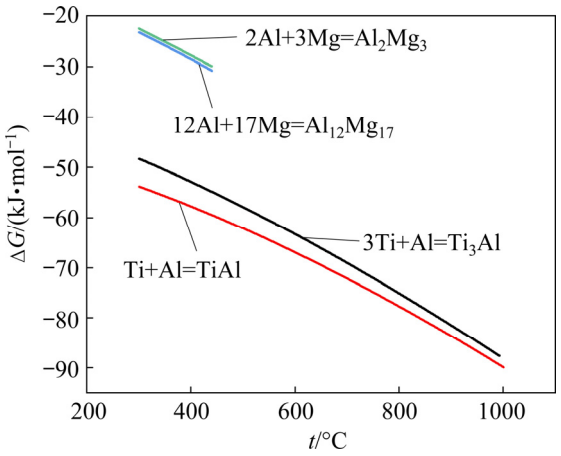

Fig. 11 Thermodynamic modelling of reactions of Al−Mg and Al−Ti systems

The heat treatment step was designed to fully dissolve the alloying elements, and 1400 °C proved to be sufficient to homogenize all the elements and obtain uniform Ti−48Al−2Cr−2Nb. Because the final product is in the powder form, compositional homogenization could ensure that each particle contains a similar composition. The XRD and elemental mapping results both demonstrated that the final composition was homogenized after the heat treatment step, but the TiAl alloy contained a large amount of oxygen (2.05%) after this step.

To better understand the deoxidation process, the phases in the high-oxygen-containing TiAl alloy were clarified. Figure 12 shows the phase diagram of the ((Ti−48Al−2Cr−2Nb)−xO) system at different temperatures calculated using Pandat software with the Ti alloy database. Evidently, the solubility of oxygen in titanium depends on the temperature, with the highest solubility (0.91% or 0.377%) at approximately 750 °C. In this study, the (Ti−48Al−2Cr−2Nb)−2.05wt.%O alloy was deoxidized at 900 °C. As shown in Fig. 12, the alloy may contain $AlNbTi_2$, Al_2O_3, and γ-TiAl phases at room temperature, whereas at 900 °C the alloy contained γ-TiAl, α_2-Ti_3Al, and some minor Al_2O_3 phases. At room temperature, some Al_2O_3 may exist in the equilibrium, but it was not detected in this study, as shown in Fig. 8. This phase is possibly absent because the final powder was furnace-cooled to room temperature in the furnace, which may prevent Al_2O_3 from forming, leading to an undetectable concentration in the powder. The $AlNbTi_2$ phase was not detected by XRD, as shown in Fig. 8, which may be due to the slow kinetics at lower temperatures during cooling.

Based on these results, the following deoxidation mechanism was proposed. First, the minor Al_2O_3 phase was reduced by Ca to form CaO and Al. The formed Al on the surface of the powder may be dissolved into the calcium to form a Ca−Al liquid. Most of Al then quickly dissolved into the TiAl alloy system to form a (TiAl+Ti_3Al)−O solid solution, which was then deoxidized by Ca to form TiAl + Ti_3Al and CaO. Equations (6)−(9) show the suggested reactions:

$$Al_2O_3+3Ca=2Al+3CaO \quad (6)$$

$$2Al+Ti_3Al-xO=3TiAl-xO \quad (7)$$

$$Ti_3Al-xO+xCa=Ti_3Al+xCaO \quad (8)$$

$$TiAl-xO+xCa=xCaO+TiAl \quad (9)$$

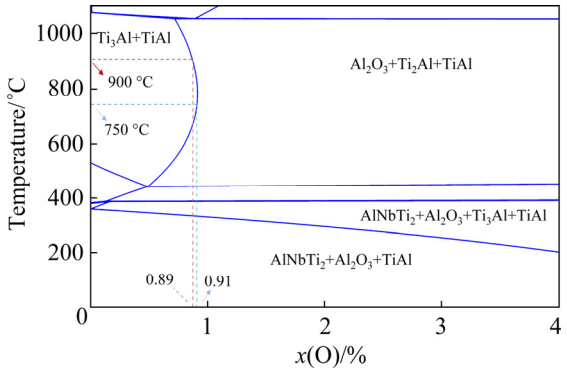

Fig. 12 Phase diagram of (Ti−48Al−2Cr−2Nb)−xO (x in mole fraction, %) produced based on Pandat software under Ti database

Our previous study demonstrated that hydrogen can destabilize the Ti−O solid solution [39−41]. To verify whether Al has a similar effect, the thermodynamic properties of (TiAl)−1 at.% O and (Ti−48Al−2Cr−2Nb)−1 at.% O systems were calculated using Pandat software with the Ti alloy database. The results are shown in Fig. 13, which reveal the effect of the Al concentration and the alloying elements of TiAl (4822) on the Gibbs free energy change (ΔG) of reaction between Ti alloy with 1 at.% O. Clearly, as the aluminum content increases, the oxygen potential decreases, which indicates that Al may similarly destabilize the titanium alloy–oxygen solid solutions. Adding Al, Cr, and Nb as alloying elements can slightly change the ΔG of the reaction, which is conducive to the deoxidation reaction.

Figure 14 illustrates the entire process on the basis of the above analysis of the reduction and

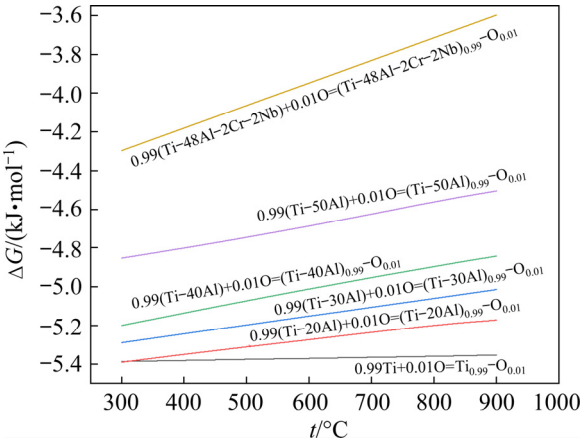

Fig. 13 Effect of Al concentration and alloying elements of TiAl (4822) on Gibbs free energy of formation of Ti−O solid solution with 1 at.% O

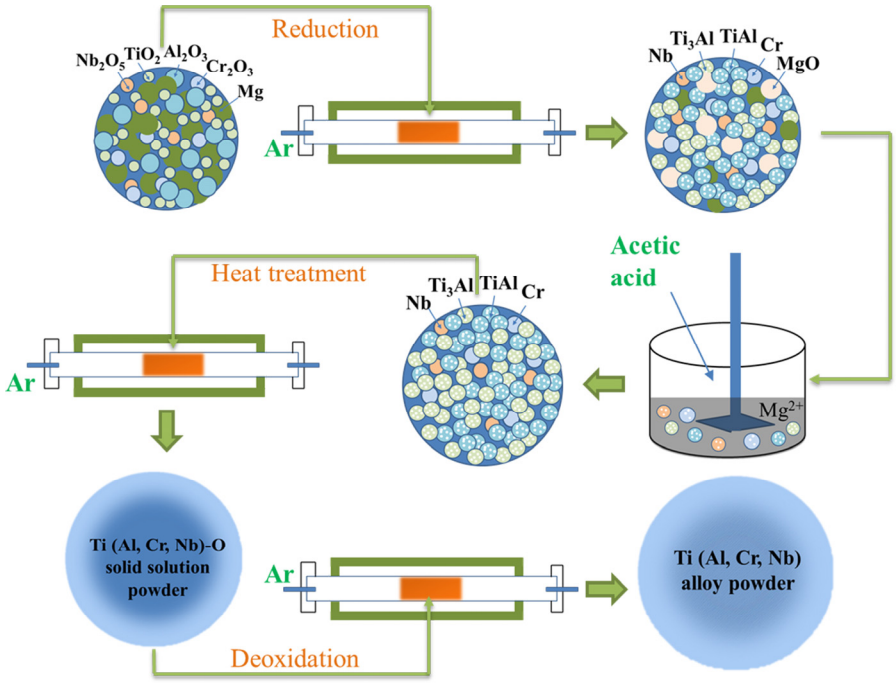

Fig. 14 Schematic diagram of Ti−48Al−2Cr−2Nb alloy preparation

deoxidation mechanisms. Specifically, the oxides of Ti, Al, Cr, and Nb were reduced by Mg, leading to the formation of Ti_3Al and TiAl, Cr, Nb, and MgO, followed by the leaching of MgO and the separation of the powder and liquid. The heat treatment step helped homogenize the entire composition and obtain homogenous Ti−48Al−2Cr−2Nb alloy with a high oxygen content. Finally, the final calcium deoxidation step removed a large amount of the remaining oxygen in the TiAl alloy powder. To the best of the authors' knowledge, this is the first report of a TiAl alloy powder with such a low oxygen content prepared through a thermochemical method.

4 Conclusions

(1) Through the direct reduction of a mixture of TiO_2, Cr_2O_3, Nb_2O_5, and Al_2O_3 powders, a Ti−48Al−2Cr−2Nb alloy powder with oxygen content of 0.057%, average particle size of 67.2 μm, and specific surface area of 0.29 m^2/g was successfully produced. The final powder contained 61.3% Ti, 30.32% Al, 2.74% Cr, and 4.73% Nb, which were homogenously distributed in the powder.

(2) The product was dense and mainly included γ-TiAl phase and some minor α_2-Ti_3Al phases. Mg was suitable for reducing such mixed oxides. Al and the remaining alloying elements destabilized the Ti−O solid solution, facilitating the deoxidation process.

(3) This study demonstrates the feasibility of preparing high purity TiAl alloy powders directly from the thermochemical process, which is a shorter process and consumes less energy, by comparing with the traditional high temperature melting and atomization powder production process.

Acknowledgments

This study was financially supported by the National Natural Science Foundation of China (No. 52004342), Innovation-driven Project of Central South University, China (No. 502501015), and the Natural Science Fund for Distinguished Young Scholar of Hunan Province, China (No. 2019JJ20031).

References

[1] DENG Guo-zhu. Titanium metallurgy [M]. Beijing: Metallurgical Industry Press, 2010. (in Chinese)

[2] WANG Hai-ling, WANG Qiang, ZENG Liang-cai, ZHANG Hai-long, DING Hong-sheng. Microstructure, mechanical and tribological performances of a directionally solidified γ-TiAl alloy [J]. Materials Characterization, 2021, 179: 111393.

[3] ISMAEEL A, WANG Cun-shan. Effect of Nb additions on microstructure and properties of γ-TiAl based alloys fabricated by selective laser melting [J]. Transactions of Nonferrous Metals Society of China, 2019, 29(5): 1007−1016.

[4] KIM Y W. Gamma titanium aluminides: Their status and future [J]. JOM, 1995, 47(7): 39−42.

[5] YAN Yong, FENG He-ping, WANG Qi, CHEN Rui-run, GUO Jing-jie, DING Hong-sheng, SU Yan-qing. Improvement of microstructure and mechanical properties of TiAl−Nb alloy by adding Fe element [J]. Transactions of Nonferrous Metals Society of China, 2020, 30(5): 1315−1324.

[6] HE Wei-wei, TANG Hui-ping, LIU Hai-yan, JIA Wen-peng, LIU Yong, YANG Xin. Microstructure and tensile properties of containerless near-isothermally forged TiAl alloy [J]. Transactions of Nonferrous Metals Society of China, 2011, 21: 2605−2609.

[7] HEIDLOFF A J, RIEKEN J R, ANDERSON I E, BYRD D, SEARS J, GLYNN M, WARD R M. Advanced gas atomization processing for Ti and Ti alloy powder manufacturing [J]. JOM, 2010, 62(5): 35−41.

[8] WU Xin-hua. Review of alloy and process development of TiAl alloys [J]. Intermetallic, 2007, 14: 10−11.

[9] HSIUNG L M, NIEH T G. Microstructures and properties of powder metallurgy TiAl alloys [J]. Materials Science and Engineering A, 2004, 364(1/2): 1−10.

[10] RAO K P, PRASAD Y, SURESH K. Hot working behavior and processing map of a γ-TiAl alloy synthesized by powder metallurgy [J]. Materials & Design, 2011, 32(10): 4874−4881.

[11] XIA Y, LUO S D, WU X, SCHAFFER G B, QIAN M. The sintering densification, microstructure and mechanical properties of gamma Ti−48Al−2Cr−2Nb alloy with a small addition of copper [J]. Materials Science and Engineering A, 2013, 559: 293−300.

[12] XIA Y, SCHAFFER G B, QIAN M. Enhanced sintering of pre-alloyed binary TiAl powder by a small addition of iron [J]. Key Engineering Materials, 2012, 520: 89−94.

[13] LIU H W, PLUCKNETT K P. Titanium aluminide (Ti−48Al) powder synthesis, size refinement and sintering [J]. Advanced Powder Technology, 2017, 28(1): 314−323.

[14] WANG Hai-ying, ZHANG Ge, YANG Fang, CAO Peng, GUO Zhi-meng, LU Bo-xin, CHEN Cun-guang, LIU Peng, VOLINSKY A A. High-density and low-interstitial Ti−23Al−17Nb prepared by vacuum pressure less sintering from blended elemental powders [J]. Vacuum, 2019, 164: 62−65.

[15] JABBAR H, COURET A, DURAND L, MONCHOUX J P. Identification of microstructural mechanisms during densification of a TiAl alloy by spark plasma sintering [J]. Journal of Alloys and Compounds, 2011, 509(41): 9826−9835.

[16] ZHAO Kun, GAO Feng. Mechanism and kinetic analysis of vacuum aluminothermic reduction for preparing TiAl intermetallics powder [J]. Journal of Alloys and Compounds, 2021, 855: 157546.

[17] LIU Cheng-cheng, LU Xin, YANG Fei, TONG Jian-bo, XU Wei, WANG Zhe, QU Xuan-hui. Preparation of TiAl alloy powder by reactive synthesis in molten KCl−LiCl salt [J]. JOM, 2018, 70: 2230−2236.

[18] SHAO Hui-ping, WANG Zhi, LIN Tao, YE Qing, GUO Zhi-meng. Preparation of TiAl alloy powder by high-energy ball milling and diffusion reaction at low temperature [J]. Rare Metals, 2018, 37: 21−25.

[19] QIU Jing-wen, FU Zheng-fan, LIU Bin, LIU Yong, YAN Jian-hui, PAN Di, ZHANG Wei-dong, BAKER I. Effects of niobium particles on the wear behavior of powder metallurgical γ-TiAl alloy in different environments [J]. Wear, 2019, 434−435: 202964.

[20] POLOZOV I, RAZUMOV N, MAKHMUTOV T, SILIN A, POPOVICH A. Synthesis of titanium orthorhombic alloy spherical powders by mechanical alloying and plasma spheroidization processes [J]. Materials Letters, 2019, 256: 126615.

[21] ZHOU Y H, LIN S F, HOU Y H, WANG D W, ZHOU P, HAN P L, LI Y L, YAN M. Layered surface structure of gas-atomized high Nb-containing TiAl powder and its impact on laser energy absorption for selective laser melting [J]. Applied Surface Science, 2018, 441: 210−217.

[22] NISHIDA M, TATEYAMA T, TOMOSHIGE R, MORITA K, CHIBA A. Electron microscopy studies of Ti−47at.%Al powder produced by plasma rotating electrode process [J]. Scripta Metallurgica et Materialia, 1992, 27(3): 335−340.

[23] GERLING R. Plasma melting inert gas atomization for production of intermetallic titanium based alloy powders [J]. Metal Powder Report, 1992, 47(11): 53.

[24] MWAMBA I A, CHOWN L H. The use of titanium hydride in blending and mechanical alloying of Ti−Al alloys [J]. Journal of the Southern African Institute of Mining and Metallurgy, 2011, 111(3): 59−165.

[25] NOVÁK P, KŘÍŽ J, PRUŠA F, KUBÁSEK J, MAREK I, MICHALCOVÁ A, VODĚROVÁ M, VOJTĚCH D. Structure and properties of Ti−Al−Si−X alloys produced by SHS method [J]. Intermetallics, 2013, 39: 11−19.

[26] BOUDEBANE S, BOUREMOUM Z, LEMBOUB S. Preparation of Ti_3Al intermetallic powder from TiO_2−Al_2O_3 oxides by calcium or magnesium reduction [J]. In Annales de Chimie Science des Materiaux, 2000, 25(5): 391−400.

[27] MAEDA M, YAHATA T, MITUGI K, IKEDA T. Aluminothermic reduction of titanium oxide [J]. Materials Transactions, JIM, 1993, 34(7): 599−603.

[28] SONG Yu-lai, DOU Zhi-he, ZHANG Ting-an, LIU Yan, NIU Li-ping. Preparation of TiAl master alloy by metallothermic reduction [J]. Rare Metal Materials and Engineering, 2020, 49(3): 1015−1019. (in Chinese)

[29] SUZUKI R O, IKEZAWA M, OKABE T H, OISHI T, ONO K. Preparation of TiAl and Ti_3Al powders by calciothermic reduction of oxides [J]. Materials Transactions, 1990, 31(1): 61−68.

[30] SUZUKI R O, SAKAMOTO H, OISHI T, ONO K. Process to produce TiAl alloy powders by calcium co-reduction from the oxide [J] Memoires et Etudes Scientifiques, Revue de Metallurgic, 1989(10): 655−658. (in French)

[31] SUZUKI R O, UEKI T, IKEZAWA M, OKABE T H, OISHI T, ONO K. A fundamental study on preparation of Al_3Ti powders by calciothermic reduction of oxides [J]. Materials Transactions, JIM, 1991, 32(3): 272−277.

[32] ROINE A. HSC 6.0 Chemistry. Chemical reactions and equilibrium software with extensive thermochemical database and flowsheet simulation [Z]. Outokumpu Research Oy Information Center, Pori, 2006.
[33] CHEN S L, DANIEL S, ZHANG F, CHANG Y A, YAN X Y, XIE F Y, OATES W A. The PANDAT software package and its applications [J]. Calphad, 2002, 26(2): 175−188.
[34] ZHANG Y, FANG Z Z, XU L, SUN P, van DEVENER B, ZHENG S L, XIA Y, LI P, ZHANG Y. Mitigation of the surface oxidation of titanium by hydrogen [J]. The Journal of Physical Chemistry C, 2018, 122(36): 20691−20700.
[35] GODLEWSKA E, KOZIŃSKI S, MANIA R, WSOŁEK M, MICHALCOVÁ A, VODĚROVÁ M, VOJTĚCH D. Manufacturing of intermetallic materials in Ti−Al and Fe−Al systems by SHS [J]. Inżynieria Materiałowa, 1998, 19(4): 929−932. (in polish)
[36] SHEN Y F, ZOU Z G, XIAO Z G, LIU K, LONG F, WU Y. Properties and electronic structures of titanium aluminides–alumina composites from in-situ SHS process [J]. Materials Science and Engineering A, 2011, 528(4/5): 2100−2105.
[37] KOPIT Y. The ability of systems based on Ni, Al and Ti to be synthesized by self-propagating high-temperature synthesis (SHS) [J]. Intermetallics, 2001, 9(5): 387−393.
[38] ZHANG Y, FANG Z Z, XIA Y, SUN P, van DEVENER B, FREE M, LEFLER H, ZHENG S L. Hydrogen assisted magnesiothermic reduction of TiO_2 [J]. Chemical Engineering Journal, 2017, 308: 299−310.
[39] XIA Y, FANG Z Z, ZHANG Y, LEFLER H, ZHANG T Y, SUN P, HUANG Z. Hydrogen assisted magnesiothermic reduction (HAMR) of commercial TiO_2 to produce titanium powder with controlled morphology and particle size [J]. Materials Transactions, 2017, 58(3): 355−360.
[40] XIA Yang, FANG Z Z, FAN De-qiu, SUN Pei, ZHANG Ying, ZHU Jun. Hydrogen enhanced thermodynamic properties and kinetics of calciothermic deoxygenation of titanium-oxygen solid solutions [J]. International Journal of Hydrogen Energy, 2018, 43: 11939−11951.
[41] ZHANG Ying, FANG Z Z, SUN Pei, ZHANG Tuo-yang, XIA Yang, ZHOU Cheng-shang, HUANG Zhe. Thermodynamic destabilization of Ti−O solid solution by H_2 and deoxygenation of Ti using Mg [J]. Journal of the American Chemical Society, 2016, 138(22): 6916−6919.

氧化物直接还原制备低氧 Ti−48Al−2Cr−2Nb 合金粉末

郭学益，董朝望，夏 阳，刘沛东，刘汉宁，田庆华

中南大学 冶金与环境学院，长沙 410083

摘 要：以 TiO_2、Al_2O_3、Nb_2O_5 和 Cr_2O_3 粉末混合物为原料，通过镁还原和钙脱氧，成功制备出氧含量低至 0.0572%、粒径<150 μm 的高纯度 Ti−48Al−2Nb−2Cr 合金粉末。详细分析了每一步产物的物相组成及元素分布。结果表明，最终粉末产品的物相为 γ-TiAl 和少量 α_2-Ti_3Al 相，Ti、Al、Cr、Nb 的原子比为 49.73:43.51:2.05:1.98，Ti、Al、Cr、Nb 均匀分布于粉末产品中。借助 HSC 化学热力学软件及 Pandat 软件下的 Ti 合金数据库，模拟研究了还原和脱氧机理。

关键词：钛铝；粉末；还原；氧化物

(Edited by Sai-qian YUAN)